CORONAL HOLES

MARTIN D. ALTSCHULER, DOROTHY E. TROTTER
High Altitude Observatory, National Center for Atmospheric Research, Boulder, Colo., U.S.A.*

and

FRANK Q. ORRALL
Institute for Astronomy, University of Hawaii, Honolulu, Hawaii, U.S.A.

(Received 25 April, 1972)

Abstract. Coronal holes are extensive regions of extremely low density in the solar corona within 60° of latitude from the equator. (They are not to be confused with the well-known coronal cavities which surround quiescent prominences beneath helmet streamers.) We have superposed maps of the calculated current-free (potential) coronal magnetic field with maps of the coronal electron density for the period of November 1966, and find that coronal holes are generally characterized by weak and diverging magnetic field lines. The chromosphere underlying the holes is extremely quiet, being free of weak plages and filaments. The existence of coronal holes clearly has important implications for the energy balance in the transition region and the solar wind.

1. Observations of Coronal Holes

On eclipse photographs and K-coronameter scans there sometimes appear coronal regions of extremely low electron density which are within 60° of latitude from the solar equator. An excellent example is the low density region seen at the southwest limb during the 7 March 1970 solar eclipse when the Sun was near maximum activity. At polar latitudes, however, low density coronal regions are quite common, particularly at times of minimum solar activity.

Low density coronal regions at low latitudes have attracted little attention until now. Since light from the corona is integrated along the line of sight and contains contributions from many coronal regions, the low density regions are not often noticed on eclipse photographs and coronameter scans unless they are sufficiently isolated in longitude from the high density regions. On the other hand, the enhanced densities of streamers are visually striking.

Recently, however, two new methods to determine the electron density distribution of the solar corona have been developed. One uses EUV disk data, the other K-coronameter limb data together with a regression analysis to overcome the difficulty of overlapping features in the line of sight.

The first method (Withbroe *et al.*, 1972) uses data of the extreme ultraviolet (EUV) spectrum (285 to 1370 Å) of the solar disk obtained by an orbiting spectrometer-spectroheliometer. An equation relating the intensity of the MgX line (625 Å) to the electron density at the base of the corona was derived for an isothermal corona (1.8×10^6 K) assuming the electron density decreases exponentially with height. With

* The National Center for Atmospheric Research is sponsored by the National Science Foundation.

Solar Physics **26** (1972) 354–365.

this equation, the measured intensity of the MgX line gives the electron density at the base of the corona probably to within a factor of two. Details of this method are found in Withbroe (1972).

The second method (Altschuler and Perry, 1972) uses K-coronameter (limb) data collected over a half solar rotation (14 days) and the assumptions that the corona is optically thin, unchanging, and rigidly rotating at the Carrington period during the time of data collection. The unknown electron density distribution is represented by a Legendre polynomial expansion and the coefficients are then determined by a least-mean-square regression analysis of the coronameter data. The electron density distribution obtained from this analysis is a function of latitude, longitude, and radial distance for the region from just above the photosphere to a solar radius above the limb ($r = 2R$). Because there is only one radial basis function in the present calculation, however, the *relative* electron density distribution that we obtain does not change with height, and our maps (we now know) are most representative of the low corona ($0.1R$ to $0.3R$ or 70 to 210 Mm above the limb). (A better solution for the radial dependence of electron density has now been achieved, and will be the subject of a later paper.) Rapid changes in the coronal density distribution in times less than that of a half solar rotation (such as might be caused by a flare or eruptive prominence) are not always detectable and may introduce error.

Since the method of Withbroe *et al.* (1972) uses data from the disk and the method of Altschuler and Perry (1972) overcomes the limb data ambiguities of overlapping coronal features in the line of sight, both of these methods can accurately indentify coronal features with the underlying chromospheric and photospheric features. Maps derived from these very different procedures reveal the existence of extensive coronal regions with extremely low electron density (typically 5 times less than the average density of the low latitude corona and 10 to 100 times less than the density of a coronal streamer). Both the EUV and K-coronameter methods agree on the disk location for the low density region seen at the southwest limb of the 7 March 1970 eclipse.

Coronal regions of low density which occur within 60° latitude from the solar equator and which extend outward from the base of the corona are called 'coronal holes' (Withbroe *et al.*, 1972; Altschuler and Perry, 1972). We distinguish a coronal hole from (1) a low density coronal region found at high latitudes near a pole and (2) a 'cavity' which occurs in a limited volume surrounding a quiescent prominence beneath a helmet streamer. A cavity is not detectable by the method of Altschuler and Perry because it usually does not extend to the first scanning height of the K-coronameter (2′ or 87 Mm above the limb) and because the simple r^{-8} radial dependence used in the present calculation is not sensitive to a positive radial gradient of electron density. (Cavities can sometimes be detected from the pB-coronameter data.)

In this paper we examine the coronal holes which were present at the time of the 12 November 1966 eclipse and compare their distribution with that of the calculated current-free coronal magnetic field. Unfortunately, satellite EUV data for the Sun are not available for November 1966.

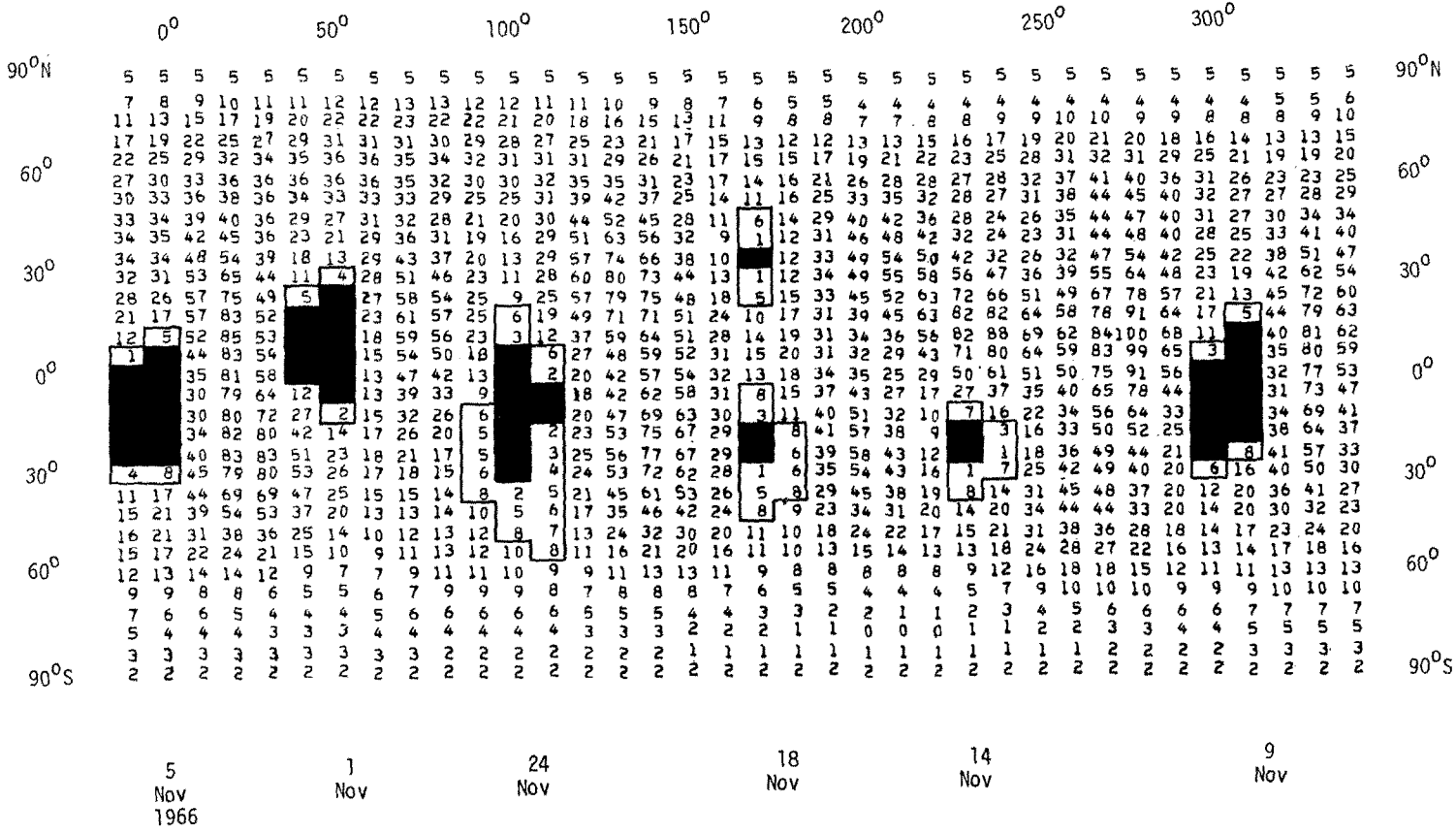

Fig. 1. Map of relative electron density of solar corona at any radius within one solar radius from the photosphere, that is, $R \leqslant r \leqslant 2\ R$ (see Figure 3 and Table I of Altschuler and Perry, 1972). The maximum density corresponds to the number 100. The solid black boxes cover the zero values of relative density within 60° of latitude from the equator; the solid contours enclose relative densities of 8 % or less within those latitudes. Carrington longitudes are used throughout.

Figure 1 is the map of the relative electron density of the solar corona of 12 November 1966 which appeared in the paper of Altschuler and Perry (1972). The maximum density, corresponding to the box labelled 100 is given as a function of height in Table I of that paper. Here, however, contours are shown for regions of low (much below average) coronal density which are within 60° latitude of the solar equator. The solid black areas are the zero values of the relative density map and correspond to coronal regions of extremely low density. The solid-line contours enclose regions with densities (at a given height) which are 8% or less of the maximum coronal density. On this particular map, we arbitrarily choose the 8% level as the boundary of a coronal hole because this level separates the coronal hole regions from the polar regions. Each of the 1116 numbers (31×36 with $\Delta\theta = 6° = 0.105$ rad and $\Delta\phi = 10° = 0.175$ rad) corresponds to a fraction $(4\pi)^{-1} \sin\theta \, \Delta\theta \, \Delta\phi = 1.465 \times 10^{-3} \sin\theta$ of the area of the entire sphere (at a given height). For the period of this map, 1 November to 20 November 1966, the coronal holes as defined by the solid contours cover 13% (and the areas in black 7%) of the solar sphere. In total, low density regions (8% or less of maximum density), including those at the solar poles, cover 18% of the area of the solar sphere (see Table I of this paper). On the other hand, high density regions

TABLE I

Area distribution for relative electron density
1 to 20 November 1966

Coronal electron density (relative scale: 0 to 100)	Area of the Sun (percent)
0 to 8	18
9 to 20	21.5
21 to 30	15
31 to 40	16
41 to 50	10
51 to 60	8
> 60	11.5

with densities exceeding 60% of the maximum density cover 11.5% (and those with densities exceeding 80% of maximum cover 3.4%) of the area of the Sun. For this data period, for latitudes within 60° of the solar equator, the coronal holes (<8% of maximum density) and the high density coronal regions (>60% of maximum density) together cover about a fourth of the area of the solar sphere.

With the improved radial dependence in the electron density maps, the coronal holes are found to extend to at least $r = 2R$ and to increase in relative area as the radial distance increases.

2. Coronal Holes and Coronal Magnetic Fields

The coronal holes seen in Figure 1 are compared with the coronal magnetic field as calculated by the potential (current-free) field method of Altschuler and Newkirk

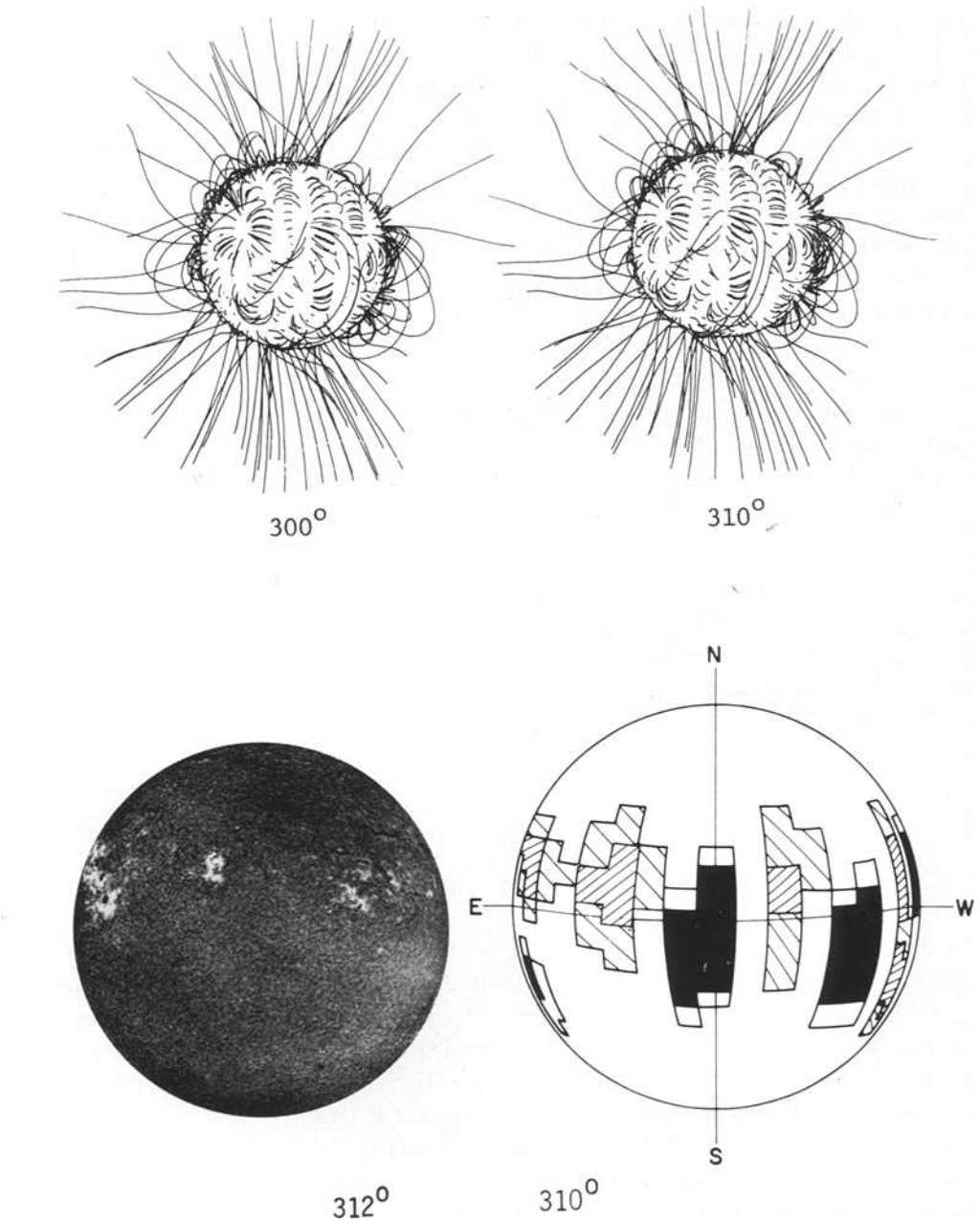

Fig. 2. Stereo view of calculated current-free (potential) coronal magnetic field, Hα photograph, and map of Figure 1 as projected on a sphere. Cross hatched regions have large electron densities.

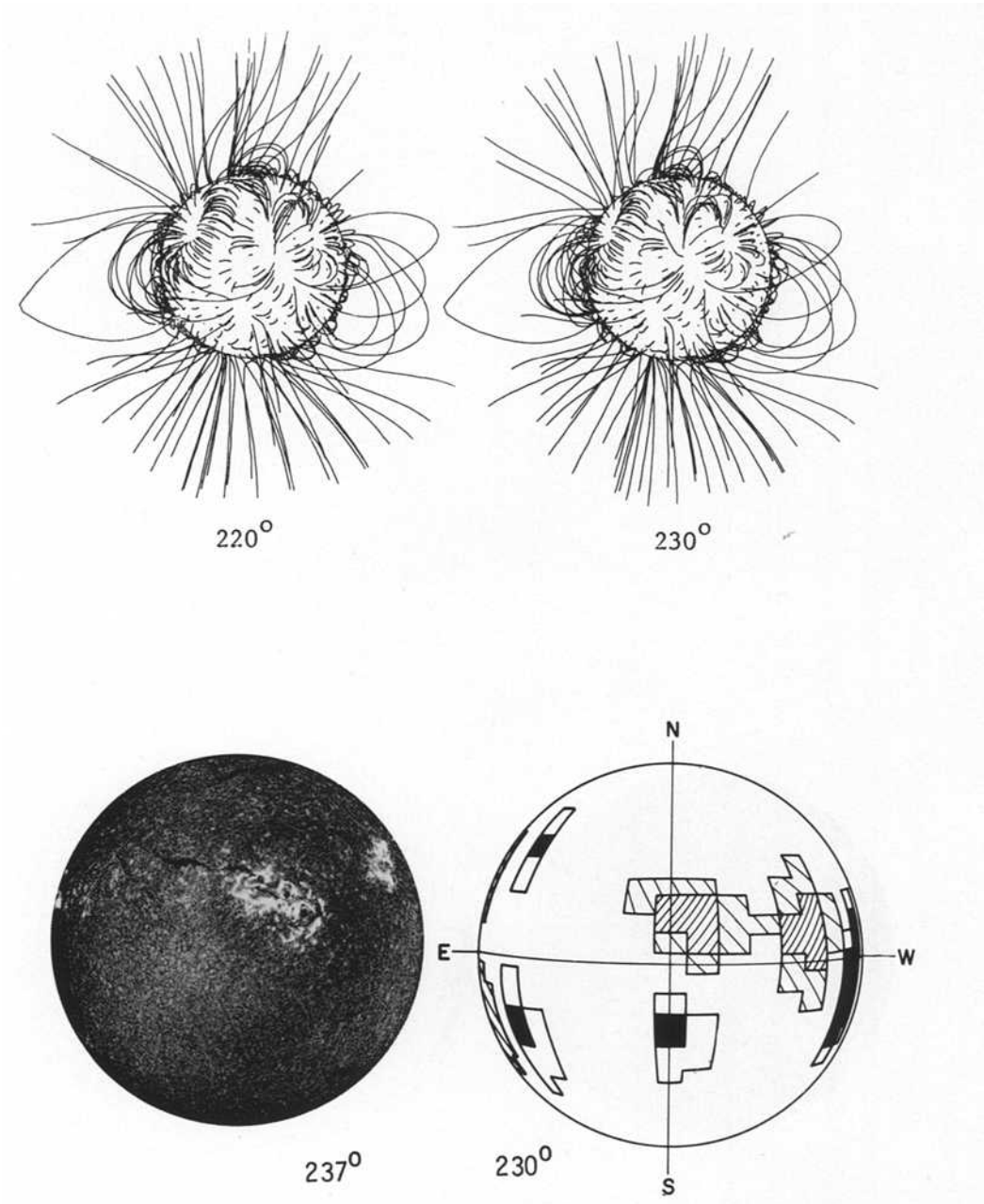

Fig. 3. Stereo view of calculated current-free (potential) coronal magnetic field, Hα photograph, and map of Figure 1 as projected on a sphere. Cross hatched regions have large electron densities.

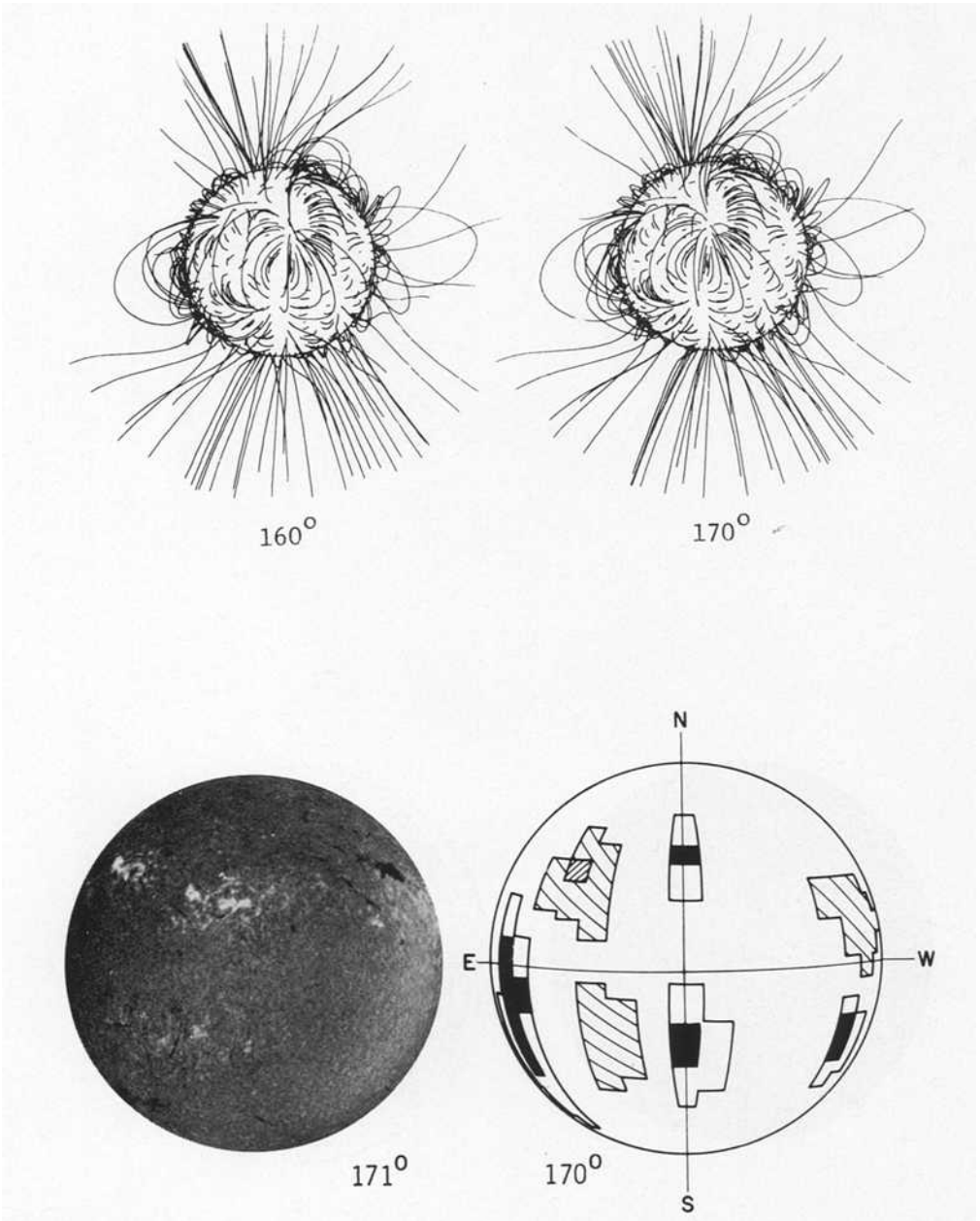

Fig. 4. Stereo view of calculated current-free (potential) coronal magnetic field, Hα photograph, and map of Figure 1 as projected on a sphere. Cross hatched regions have large electron densities.

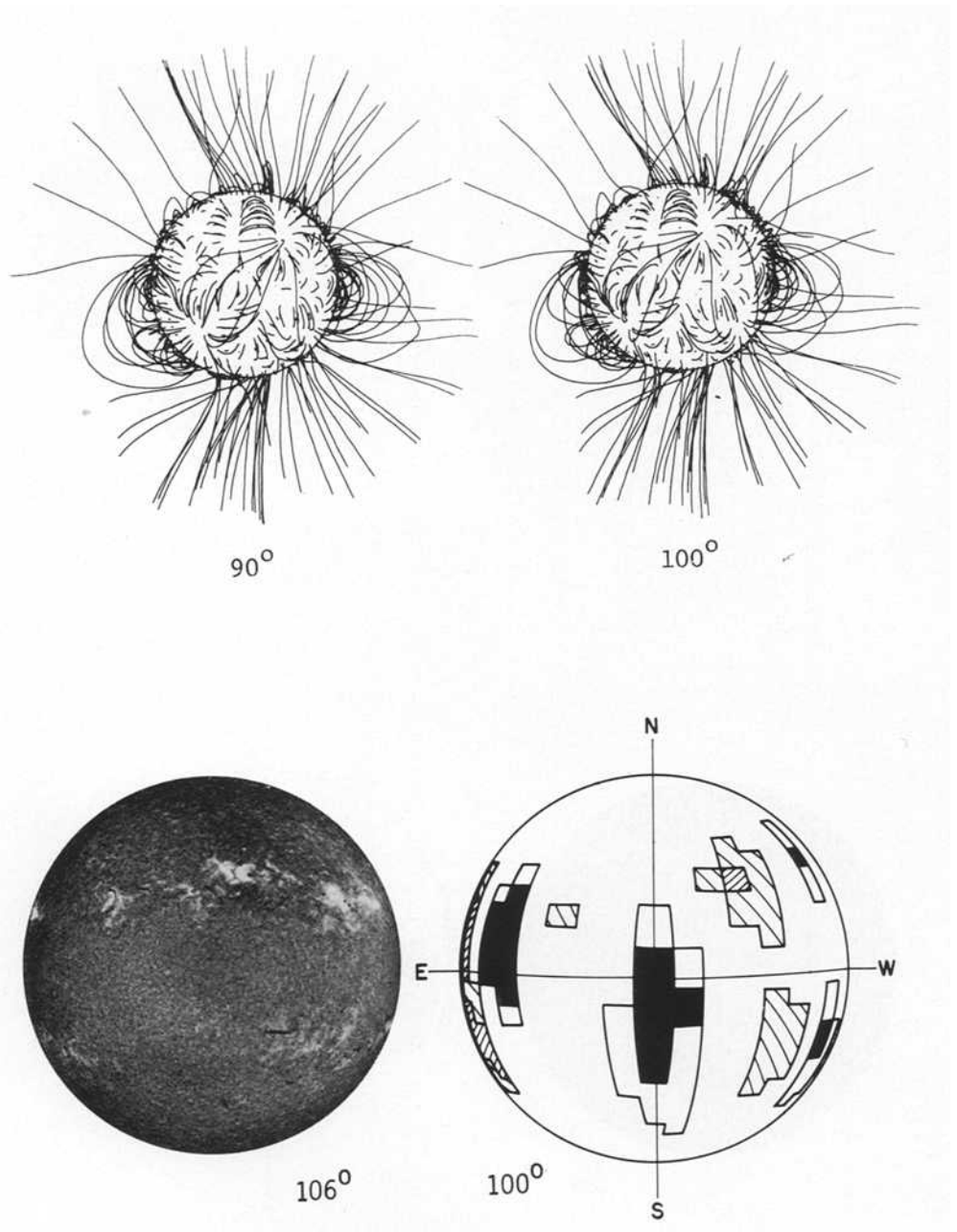

Fig. 5. Stereo view of calculated current-free (potential) coronal magnetic field, Hα photograph, and map of Figure 1 as projected on a sphere. Cross hatched regions have large electron densities.

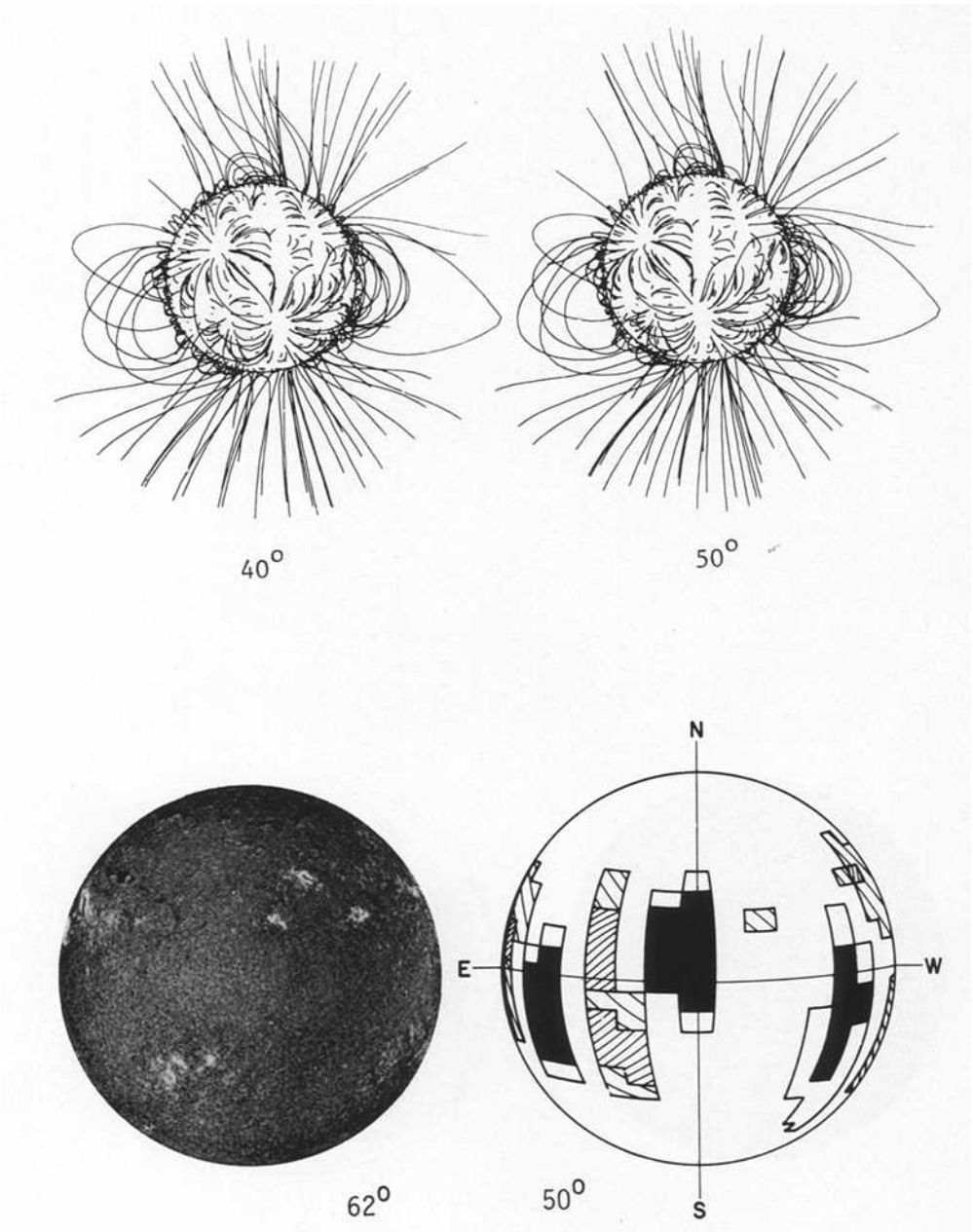

Fig. 6. Stereo view of calculated current-free (potential) coronal magnetic field, Hα photograph, and map of Figure 1 as projected on a sphere. Cross hatched regions have large electron densities.

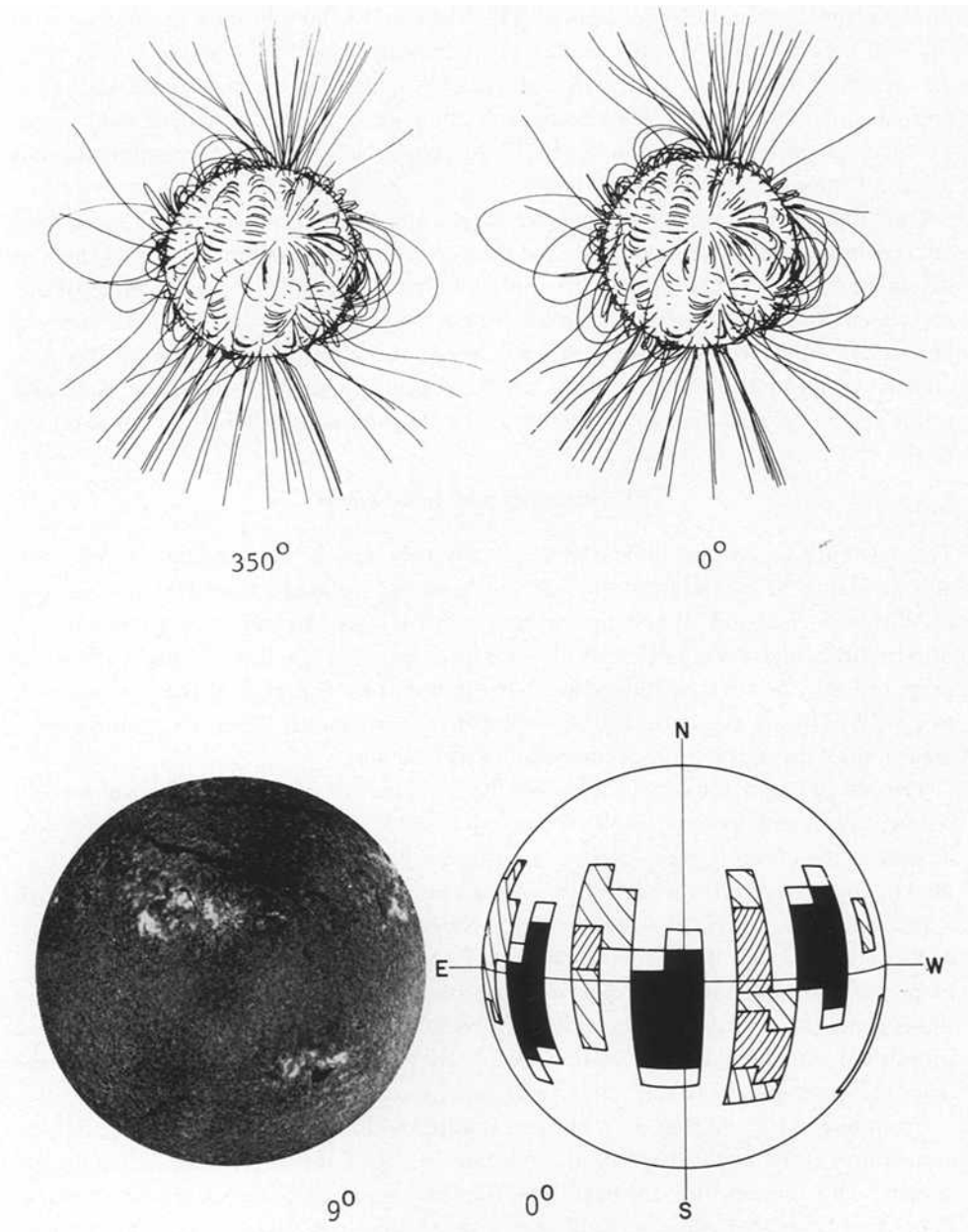

Fig. 7. Stereo view of calculated current-free (potential) coronal magnetic field, Hα photograph, and map of Figure 1 as projected on a sphere. Cross hatched regions have large electron densities.

(1969). Figures 2 through 7 show the coronal holes of Figure 1 projected onto the photosphere in spherical coordinates. The black and solid contours are the same as those in Figure 1; the cross hatched areas are beneath regions of high coronal density. To the left of the coronal hole map is an Hα photograph for the same time. Above the coronal hole map and the Hα photograph are a stereo pair of magnetic field maps. By relaxing the eye muscles, one should be able to see a stereo (three-dimensional) image of the magnetic field lines.

Our impression from these magnetic maps (and from those calculated for strong field regions but not shown here) is that the coronal holes generally occur in weak and diverging magnetic field regions. The only coronal hole (of the 7 distinct holes of our set) which possesses a relatively large amount of magnetic flux is the one in the northern hemisphere at Carrington longitude 170°. Some of the flux emanating from this hole appears connected to the hole in the southern hemisphere at the same meridian and to the region between the (southern) coronal hole and the high density coronal region to the east.

3. Summary and Conclusions

The existence of coronal holes, that is, extremely low density regions in the solar corona within 60° of the solar equator, has been established by the EUV observations of Withbroe *et al.* (1972) and by the analysis of K-coronameter data by the method of Altschuler and Perry (1972). With an improvement of the latter method (paper in preparation), the coronal holes have been traced from the base of the corona $r = R$ to $r = 2R$. During the period 1 November to 20 November 1966, the photospheric area underlying coronal holes covered 13% of the Sun.

The physics of coronal holes involves the dynamics of both the chromosphere and corona. The observations of Withbroe *et al.* (1972) show that the holes have low density in the chromosphere-corona transition region at the base of the corona. Both the Hα photographs (from Sacramento Peak Observatory) shown in Figures 2 through 7 and the K line (CaII) photographs for this period (from Osservatorio Astronomico di Roma) show that the coronal holes occur above quiet chromospheric regions free of plages and filaments. The quiet chromospheric regions, however, are larger than the coronal holes, and with the rather low resolution photographs that we have, we cannot see whether the quiet chromosphere underlying the coronal holes is different from the quiet chromosphere underlying nearby coronal regions of normal density.

From our work and that of Withbroe, it appears that in a coronal hole the density and temperature at the base of the corona and thus the coronal scale height are smaller. This suggests that the heating of the corona and chromosphere is less efficient in coronal holes, but since the field lines diverge, that losses by heat conduction may be significant. However, Withbroe points out that heat conduction is proportional to the square of the electron pressure, which is very low in the coronal holes. Thus it appears that the coronal heating is indeed less efficient in the coronal holes.

Osterbrock (1961) and Kuperus (1965) argued that the intense magnetic fields of active regions should increase the flux of mechanical energy into the corona, thereby

causing higher temperatures above active regions and an increase of density and mass flux in the corona. Pneuman (1968, 1969) argued that the coronal field can produce density enhancements similar to coronal streamers even if there is no field modulation of the mechanical energy input. Newkirk and Altschuler (1970), Bohlin (1970), and Hansen *et al.* (1971) found that denser coronal regions are indeed correlated with stronger coronal magnetic fields. Here we have shown that cooler and more tenuous coronal regions are generally associated with weak and open magnetic field structures. Apparently, if there is a coronal hole, the magnetic field diverges; however, the converse is not always true since coronal condensations can also occur above diverging fields (Newkirk and Altschuler, 1970).

In summary, coronal holes occur over quiet chromospheric regions where there is usually a weak and diverging magnetic field. We suggest that coronal holes are regions of reduced chromospheric and coronal heating, and predict that the chromospheric fine structure underlying them will be found to differ from that below nearby coronal regions of average density. Clearly many more observations of the corona, chromosphere, and associated magnetic fields will be required to understand the nature of coronal holes.

Acknowledgements

We thank R. Hansen, S. Hansen and C. Garcia for the coronagraph data and R. Howard (Hale Observatories) for the photospheric magnetic field data. The latter data were taken by R. Howard with the support of the Office of Naval Research. We are grateful to G. Withbroe (Harvard) and G. Pneuman for invaluable discussions. The research of one of us (F.Q.O.) was supported by NASA Grant NGL 12-001-011.

References

Altschuler, M. D. and Newkirk, G.: 1969, *Solar Phys.* **9**, 131.
Altschuler, M. D. and Perry, R. M.: 1972, *Solar Phys.* **23**, 410.
Bohlin, J. D.: 1970, *Solar Phys.* **13**, 153.
Hansen, R. T., Hansen, S. F., Garcia, C. J., and Trotter, D. E.: 1971, *Solar Phys.* **18**, 271.
Kuperus, M.: 1965, *Res. Astron. Obs. Utrecht* **17** (1), 1.
Newkirk, G. and Altschuler, M. D.: 1970, *Solar Phys.* **13**, 131.
Osterbrock, D. E.: 1961, *Astrophys. J.* **134**, 347.
Pneuman, G. W.: 1968, *Solar Phys.* **3**, 578.
Pneuman, G. W.: 1969, *Solar Phys.* **6**, 255.
Withbroe, G. L.: 1972, *Solar Phys.*, in press.
Withbroe, G. L., Dupree, A. K., Goldberg, L., Huber, M. C. E., Noyes, R. W., Parkinson, W. H., and Reeves, E. M.: 1972, *Solar Phys.* **21**, 272.